



Available online at www.sciencedirect.com

ScienceDirect

Comput. Methods Appl. Mech. Engrg. 366 (2020) 112980

Computer methods in applied mechanics and engineering

www.elsevier.com/locate/cma

Quadrilateral mesh generation II: Meromorphic quartic differentials and Abel–Jacobi condition

Na Lei^{a,c,d}, Xiaopeng Zheng^{a,c,d,*}, Zhongxuan Luo^{a,c,d}, Feng Luo^e, Xianfeng Gu^b

^a Dalian University of Technology, Dalian, China

^b Stony Brook University, NY, US

^c Key Laboratory for Ubiquitous Network and Service Software of Liaoning Province, Dalian, China

^d DUT-RU Co-Research Center of Advanced ICT for Active Life, Dalian, China

^e Rutgers University, NJ, US

Received 24 June 2019; received in revised form 1 March 2020; accepted 1 March 2020 Available online xxxx

Abstract

This work discovers the equivalence relation between quadrilateral meshes and meromorphic quartic differentials. Each quad-mesh induces a conformal structure of the surface, and a meromorphic quartic differential, where the configuration of singular vertices corresponds to the configurations of the poles and zeros (divisor) of the meromorphic differential. Due to Riemann surface theory, the configuration of singularities of a quad-mesh satisfies the Abel–Jacobi condition. Inversely, if a divisor satisfies the Abel–Jacobi condition, then there exists a meromorphic quartic differential whose divisor equals the given one. Furthermore, if the meromorphic quartic differential is with finite trajectories, then it also induces a quad-mesh, the poles and zeros of the meromorphic differential correspond to the singular vertices of the quad-mesh.

Besides the theoretic proofs, the computational algorithm for verification of Abel–Jacobi condition is also explained in detail. Furthermore, constructive algorithm of meromorphic quartic differential on genus zero surfaces is proposed, which is based on the global algebraic representation of meromorphic differentials.

Our experimental results demonstrate the efficiency and efficacy of the algorithm. This opens up a novel direction for quad-mesh generation using algebraic geometric approach. © 2020 Elsevier B.V. All rights reserved.

Keywords: Quadrilateral mesh; Meromorphic quartic differential; Abel-Jacobi condition; Algebraic geometry; Singularity distribution

1. Introduction

1.1. Motivation

Quadrilateral meshes play a fundamental role in computational mechanics, geometric modeling, computer aided design, animation, digital geometry processing and many fields. Despite tens of years' research efforts, rigorous and automatic algorithms to produce high quality quad-meshes have not been achieved yet. The theoretic understanding

^{*} Corresponding author at: Dalian University of Technology, Dalian, China. *E-mail address:* zhengxp@dlut.edu.cn (X. Zheng).

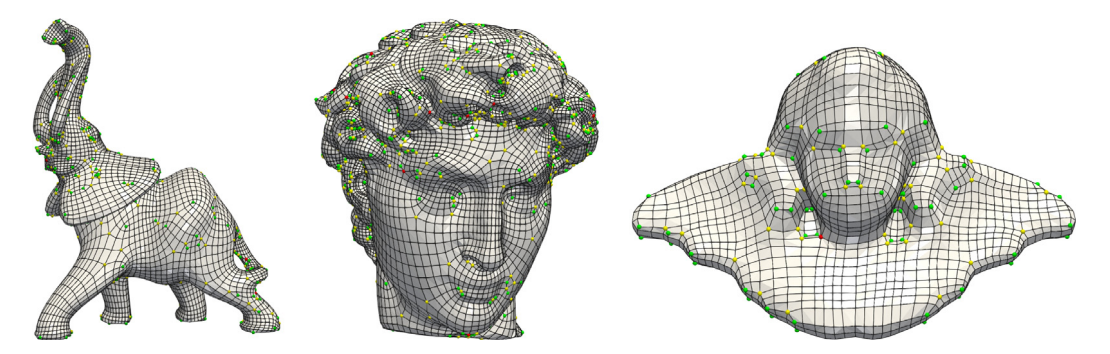


Fig. 1. Quadrilateral meshes with singularities on them, green, yellow and red dots represent singularities with valencies 3, 5 and 6 respectively. (For interpretation of the references to color in this figure legend, the reader is referred to the web version of this article.)

of the singularity configurations (the locations and valences) still remains preliminary. This work focuses on giving sufficient and necessary conditions for singularity configurations based on Riemann surface theory (see Fig. 1).

More specifically, given a closed surface Σ embedded in the Euclidean space \mathbb{R}^3 , it has the induced Euclidean Riemannian metric **g**. Suppose the surface is tessellated by a quadrilateral mesh \mathcal{Q} . If a vertex in \mathcal{Q} with topological valence 4, then the vertex is *regular*, otherwise *singular*. The singularity configuration of \mathcal{Q} is represented as the *divisor* of \mathcal{Q} , defined as

$$D_{\mathcal{Q}} := \sum_{v \in \mathcal{Q}} (k(v) - 4)v,\tag{1}$$

where v is a vertex of Q, k(v) is the topological valence of v. The goal of this work is to find the necessary and sufficient conditions for quad-mesh divisors.

1.2. Quad-mesh induced structures

A quad-mesh Q naturally induces several structures, each of them gives some information about the singularity configuration. The induced conformal structure gives the most fundamental and complete information.

Combinatorial structure. Suppose the number of vertices, edges, faces of Q are V, E, F, then E = 2F, $\sum kn_k = 4F$, $\sum n_k = V$, where n_k is the number of vertices with valence k, furthermore Euler formula holds, $V + F - E = \chi(\Sigma)$, where $\chi(\Sigma)$ is the Euler characteristic number of Σ .

Riemannian metric structure. This part is to discuss Riemannian metric structure, and the reader can refer to paper [1]. If each face of Q is treated as the unit planar square, a flat Riemannian metric with cone singularities is induced, denoted as \mathbf{g}_Q . A vertex with k-valence has discrete curvature $\frac{4-k}{2}\pi$. the Gauss-Bonnet condition shows the total curvature equals the product of 2π and the Euler characteristic number $\chi(\Sigma)$. This implies

$$\sum_{v \in Q} (k(v) - 4) = -4\chi(\Sigma). \tag{2}$$

The degree of the divisor (defined in Section 3) also satisfies the equation above.

The holonomy group induced by the metric \mathbf{g}_Q on the surface with punctures at the singular vertices is the rotation group

$$\{e^{i\frac{\pi}{2}k}, k \in \mathbb{Z}\}. \tag{3}$$

This is the so-called *holonomy condition*. Furthermore, if we connect the horizontal and vertical edges of the quadfaces, we get geodesic loops. If we subdivide the quad-mesh infinitely many times, we obtain geodesic lamination, each leaf is a closed loop. This is called the *finite geodesic lamination condition* [1].

Conformal structure. In this work, we show that the quad-mesh Q induces a conformal structure, and can be treated as a Riemann surface S_Q . Furthermore, it induces a meromorphic quartic differential ω_Q , whose trajectories are finite. Naturally the quad-mesh divisor D_Q is equivalent to the divisor D of ω_Q . By Abel theorem, the divisor satisfies the Abel–Jacobi condition in Eq. (8). Inversely, if a point configuration \tilde{D} satisfies the Abel–Jacobi condition, then there must be a meromorphic quartic differential ω , whose divisor D equals \tilde{D} . If the trajectories of ω are finite, then ω induces a quad-mesh.

Comparison between structures. The metric structure \mathbf{g}_Q gives partial information about the divisor D_Q ; whereas the conformal structure S_Q and the meromorphic quartic differential ω_Q gives more thorough information about D_Q .

Given any divisor $D = \sum_k n_k p_k$, where n_k is an integer, and the total number of p_k 's is finite (refer to Section 3). If $\sum n_k = -4\chi(\Sigma)$, then one can construct a flat Riemannian metric conformal to the original metric using Ricci flow [2]. The flat metric is with cone singularities at p_k , where the angle equals $\pi(n_k + 4)/2$. But this flat metric may not satisfy the holonomy condition in Eq. (3). If furthermore the divisor D satisfies the Abel–Jacobi condition, then the obtained flat metric satisfies the holonomy condition.

We use a simple example to demonstrate the power of Abel–Jacobi condition. The following question is raised in [3]:

Problem 1.1. Is there a quad-mesh on a closed torus, such that it has only two singularities, one valence 3 vertex and one valence 5 vertex, other vertices are regular (with valence 4)?

From heuristic experiments, it seems that such a quad-mesh does not exist. But it is difficult to find a rigorous argument: from topological point of view, the connectivity satisfies the Euler equation; from geometric point of view, there exists a flat Riemannian metric with the two cone singularities with curvature $\pi/2$ and $-\pi/2$ corresponding to the valence 3 and valence 5 vertices. But by Abel–Jacobi condition, we can show such kind of quad-mesh does not exist in Corollary 4.12.

1.3. Contributions

This work opens a novel direction for quad-mesh generation based on Riemann surface theory:

- 1. To the best of our knowledge, this is the first work that discovers the intrinsic connection between quadrilateral meshes and meromorphic quartic differentials (Theorems 4.7 and 4.8).
- 2. This work gives the necessary and sufficient conditions for the singularity configuration, i.e. the Abel–Jacobi conditions for divisors (Theorem 4.11) and an algorithm to check the validity of the quantity and distribution of the singularities.
- 3. This work proposes to generate a quad-mesh by constructing the corresponding meromorphic quartic differential with global algebraic representation.

The work is organized as follows: Section 2 briefly reviews the most related works; Section 3 introduces the theoretic background, Section 4 proves the equivalence between quad-meshes and meromorphic quartic differentials, Abel–Jacobi conditions; Section 5.2 explains the algorithm in detail, and gives simple examples to verify Abel–Jacobi conditions and construct meromorphic quartic differentials; finally, the work concludes in Section 6.

2. Previous works

There are many approaches for quadrilateral mesh generation, a thorough survey can be found in [4]. In the following, we only briefly mention the most related works.

Triangle mesh conversion. Quad-meshes can be generated by conversion from triangular meshes directly. The simplest way is to insert the barycenters of faces and edges to obtain the initial quad-mesh, then perform Catmull–Clark subdivision. Alternatively, two original adjacent triangles can be fused into one quadrilateral to form a quad-mesh [5–8]. This approach can only produce unstructured quad-meshes, the quad-mesh quality is determined by the input triangle mesh.

Patch based approach. This approach computes the coarsest level quadrilateral tessellation first, where the cutting graph is called the skeleton, then coarse mesh is subdivided to obtain finer level quad-meshes. The skeleton can be generated by clustering method, which merges neighboring triangles into a patch, including normal-based and center-based methods [9,10]. Another method is to deform the input surface into a polycube shape, which is the union of cubes, then the faces of the polycube give the patches [11–14]. This approach can generated semi-regular quad-meshes.

Parameterization based approach. Parameterization based approach computes the quadrilateral tessellation in the parameter domain, or finds the skeleton from intrinsic geometric functions or differentials. The spectral surface quadrangulation method [15,16] produces the skeleton structure from the Morse–Smale complex of an eigenfunction of the Laplacian operator on the input mesh. Discrete harmonic forms [17], periodic Global Parameterization [18] and Branched Coverings method [19] are all based on parameterization for quad mesh generation.

Voronoi based method. Centroidal Voronoi Tessellation (CVT) produces a surface cell decomposition with uniform cell sizes and shapes. The method in [20] generalizes the CVT from L^2 distance to general L^p distance, when p goes to infinity, the cells tend to be quadrilateral, this method allows for aligning the axes of the Voronoi cells with a predefined background tensor field. This method can only produce non-structured quad-mesh.

Cross field based approach. Cross field based approach has close relationship with parameterization based approach, and it can be used in the computation of parameterization. Since cross field guided quad-mesh generation is one of the most popular approach, we review the most related approaches here. Each algorithm first chooses a way to represent a cross, for example N-RoSy representation [21], period jump technique [22] and complex value representation [23]; then the algorithm usually generates a smooth cross field by energy minimization technique, such as discrete Dirichlet energy optimization [24]. In the end, based on the obtained cross field, these approaches generate the quad meshes by using streamline tracing techniques [25] or parameterization method [4]. The cross field guided quad mesh generation method can be very useful and flexible. However it is difficult to control the position of the singularities and the structures of the quad layout directly. Cross-fields also suffer from being just direction fields, meaning that their scaling can be far from accurate.

The work in [26] relates the Ginzburg–Landau theory with the cross field for genus zero surface case. This work further generalizes the work in [26] by relating Riemann surface theory with the cross fields for surfaces with arbitrary topologies. In theory, cross field gives the horizontal/vertical directions of a meromorphic quartic differential, but ignores the amplitude. Therefore, a meromorphic differential is a more precise representation of a quad-mesh.

Metric based approach. A quad-mesh induces a flat metric with cone singularities. Furthermore, the work in [1] shows the holonomy group of the metric has special properties. Therefore the method in [1] proposes to construct a flat metric using Ricci flow algorithm with singularities at the given points, such that a quad-mesh can be induced when the holonomy conditions are met. The existence of the solution to the Ricci flow has theoretic guarantees. However the holonomy condition heavily depends on the singularity configuration. The work in [1] did not answer when the singularity configurations are appropriate for the holonomy condition.

In contrast, the current work gives the sufficient and necessary condition for the singularity configuration in order to satisfy the holonomy requirements: the Abel–Jacobi condition.

Holomorphic differential approach. In [27] and [28], the holomorphic quadratic differential is utilized to generate quad-meshes and hex-meshes, this approach produces quad-meshes with least singularities and highest smoothness. However, this approach cannot model singularities with odd topological valences, which greatly prevents the method for general applications in practice.

The current work is a direct generalization of this approach, by generalizing holomorphic quadratic differentials to more general meromorphic quartic differentials. This conquers the difficulties raised in the holomorphic differential method, and covers all possible quad-meshes.

Comparing with all existing approaches, current work shows the equivalence between quad-meshes and meromorphic quartic differentials, and gives the Abel–Jacobi condition for singularities. This picture is most general and complete, generalizes most existing approaches including cross fields, Strebel differential and metric based methods.

3. Theoretic background

This section briefly reviews the basic concepts and theorems in Riemann surface theory, details can be found in [29].

3.1. Riemann surface

Definition 3.1 (Topological Manifold). Suppose Σ is a topological space, $\{U_{\alpha}\}$ is a family of open sets covering the space, $\Sigma \subset \bigcup_{\alpha} U_{\alpha}$. For each open set U_{α} , there exists a homeomorphism $\varphi_{\alpha}: U_{\alpha} \to \mathbb{R}^{n}$, the pair $(U_{\alpha}, \varphi_{\alpha})$ is called a local chart. The collection of local charts form the atlas of M, $\mathcal{A} = \{(U_{\alpha}, \varphi_{\alpha})\}$. For any pair of open sets, U_{α} and U_{β} , if $U_{\alpha} \cap U_{\beta} \neq \emptyset$, the transition map is given by $\varphi_{\alpha\beta}: \varphi_{\alpha}(U_{\alpha} \cap U_{\beta}) \to \varphi_{\beta}(U_{\alpha} \cap U_{\beta}), \varphi_{\alpha\beta} = \varphi_{\beta} \circ \varphi_{\alpha}^{-1}$. Then Σ is called a closed n-dimensional manifold.

Two dimensional manifolds are called surfaces.

Definition 3.2 (Conformal Atlas). Suppose S is a two dimensional topological manifold, equipped with an atlas $A = \{(U_{\alpha}, \varphi_{\alpha})\}$, every local chart is complex coordinate $\varphi_{\alpha} : U_{\alpha} \to \mathbb{C}$, denoted as z_{α} , and every transition map is biholomorphic,

$$\varphi_{\alpha\beta}: \varphi_{\alpha}(U_{\alpha} \cap U_{\beta}) \to \varphi_{\beta}(U_{\alpha} \cap U_{\beta}), \quad z_{\alpha} \mapsto z_{\beta},$$

then the atlas is called a conformal atlas.

Definition 3.3 (*Riemann Surface*). A topological surface with a conformal atlas is called a Riemann surface.

Definition 3.4 (Biholomorphic Map). Suppose $f:(S,\{(U_{\alpha},\varphi_{\alpha})\})$ to $(T,\{(V_{\beta},\psi_{\beta})\})$ is a map between two Riemann surfaces, if every local representation

$$\psi_{\beta} \circ f \circ \varphi_{\alpha}^{-1} : \varphi_{\alpha}(U_{\alpha}) \to \psi_{\beta}(V_{\beta})$$

is biholomorphic, then f is called a biholomorphic map between Riemann surfaces, namely a conformal map.

Suppose (S, \mathbf{g}) is an oriented surface with a Riemannian metric \mathbf{g} . For each point $p \in \Sigma$, we can find a neighborhood U(p), inside U(p) the *isothermal coordinates* (u, v) can be constructed, such that $\mathbf{g} = e^{2\lambda(u,v)}(du^2 + dv^2)$. The atlas formed by all the isothermal coordinates is a conformal atlas, therefore the surface (S, \mathbf{g}) is a Riemann surface:

Theorem 3.5. All oriented surfaces with Riemannian metrics are Riemann surfaces.

Two metrics \mathbf{g}_1 , \mathbf{g}_2 on a surface Σ are *conformal equivalent* to each other, if there is a scalar function $\lambda: S \to \mathbb{R}$, such that $\mathbf{g}_1 = e^{2\lambda}\mathbf{g}_2$.

3.2. Meromorphic functions and differentials

Definition 3.6 (*Holomorphic Function*). Suppose $f: \mathbb{C} \to \mathbb{C}$ is a complex function defined on \mathbb{C} , $(x, y) \mapsto (u(x, y), v(x, y))$, if the function satisfies the conditions below:

- $\frac{\partial u}{\partial x}$, $\frac{\partial u}{\partial y}$, $\frac{\partial v}{\partial x}$, $\frac{\partial v}{\partial y}$ exist everywhere on \mathbb{C} ;
- ullet f satisfies the Cauchy–Riemann equations everywhere on $\mathbb C$

$$\frac{\partial u}{\partial x} = \frac{\partial v}{\partial y}, \quad \frac{\partial u}{\partial y} = -\frac{\partial v}{\partial x},$$

- f is continuous in \mathbb{C} ;
- $\frac{\partial u}{\partial x}$, $\frac{\partial u}{\partial y}$, $\frac{\partial v}{\partial x}$, $\frac{\partial v}{\partial y}$ are continuous on \mathbb{C} .

then f is called a holomorphic function on \mathbb{C} . If f is invertible, furthermore f^{-1} is also holomorphic, then f is called biholomorphic.



Fig. 2. Zeros on holomorphic 1-forms on a genus two surface.

Definition 3.7 (*Meromorphic Function*). Suppose $f: \mathbb{C} \to \mathbb{C} \cup \{\infty\}$ is a complex function, f(z) = p(z)/q(z), where p(z) and q(z) are holomorphic functions, then f(z) is called a meromorphic function.

Definition 3.8 (Laurent Series). The Laurent series of a meromorphic function about a point z_0 is given by

$$f(z) = \sum_{n=k}^{\infty} a_n (z - z_0)^n,$$

the series $\sum_{k\geq 0}^{\infty} a_n (z-z_0)^n$ is called the analytic part of the Laurent series; the series $\sum_{n<0} a_n (z-z_0)^n$ is called the principal part of the Laurent series. a_{-1} is called the residue of f at z_0 .

Definition 3.9 (Zeros and Poles). Given a meromorphic function f(z), its Laurent series at point $p \in \mathbb{C}$ has the form

$$f(z) = \sum_{n=k}^{\infty} a_n (z - p)^n,$$

where k is finite. if k > 0, then p is a zero point of order k; if k < 0, then p is called a finite pole of f(z) of order k; if k = 0, then p is called a regular point whose order is 0. The order k of a zero or a pole at the point p of f is denoted as $v_p(f)$.

The concepts of holomorphic and meromorphic functions can be generalized to Riemann surfaces.

Definition 3.10 (*Meromorphic Function on Riemann Surface*). Suppose a Riemann surface $(S, \{(U_\alpha, z_\alpha)\})$ is given. A complex function is defined on the surface $f: S \to \mathbb{C} \cup \{\infty\}$. If on each local chart (U_α, z_α) , the local representation of the functions $f \circ \varphi_\alpha^{-1} : \mathbb{C} \to \mathbb{C} \cup \{\infty\}$ is meromorphic, then f is called a meromorphic function defined on S.

A meromorphic function can be treated as a holomorphic map from the Riemann surface to the unit sphere.

Definition 3.11 (*Meromorphic Differential*). Given a Riemann surface $(S, \{z_{\alpha}\})$, ω is a meromorphic differential of order n, if it has local representation,

$$\omega = f_{\alpha}(z_{\alpha})(dz_{\alpha})^{n}$$

where $f_{\alpha}(z_{\alpha})$ is a meromorphic function, n is an integer; if $f_{\alpha}(z_{\alpha})$ is a holomorphic function, then ω is called a holomorphic differential of order n.

A holomorphic differential of order 1 is called a *holomorphic 1-form* (see Fig. 2); A holomorphic differential of order 2 is called a *holomorphic quadratic differential*; A meromorphic differential of order 4 is called a *meromorphic quartic differential*.



Fig. 3. Horizontal trajectories of holomorphic quadratic differentials.

Definition 3.12 (Zeros and Poles of Meromorphic Differentials). Given a Riemann surface $(S, \{z_{\alpha}\})$, ω is a meromorphic differential with local representation,

$$\omega = f_{\alpha}(z_{\alpha})(dz_{\alpha})^{n}.$$

If z_{α} is a pole (or a zero) of f_{α} with order k, then z_{α} is called a pole (or a zero) of the meromorphic differential ω of order k.

We use $Sing_{\omega}$ to denote the singularity set of ω which is the set of poles and zeros. Locally near a regular point p, the differential $\omega = f(z)(dz)^n$ can be represented as the nth power of a 1-form h(z)dz where $h^n(z) = f(z)$ and thus $h(z) = \sqrt[n]{f(z)}$ coincides with one of n possible branches of the nth root. We call this n-valued 1-form the nth roots of ω , which is a globally well-defined multi-valued meromorphic 1-form on S.

Definition 3.13 (*Trajectories of Meromorphic Differentials*). Given a meromorphic *n*-differential ω on *S* we define *n* distinct line fields on $S \setminus Sing_{\omega}$ as follows. At each non-singular point *z* there are exactly *n* distinguished directions dz at which $\omega = f(z)(dz)^n$ attains real values. Integral curves of these line fields are called trajectories of ω .

Suppose ω is a meromorphic quadratic differential, dz is a horizontal (vertical) direction if f(z) is real and $f(z)(dz)^2 > 0$ ($f(z)(dz)^2 < 0$). Integral curves of horizontal direction are called horizontal (vertical) trajectories.

Definition 3.14 (*Strebel Differential*). A meromorphic quadratic differential is called a Strebel differential, if all its horizontal trajectories are finite.

Fig. 3 shows the horizontal trajectories of Strebel differentials. Note that the vertical trajectories of a Strebel differential may not necessarily be finite.

3.3. Divisor

Definition 3.15 (*Divisor*). The Abelian group freely generated by points on a Riemann surface is called the divisor group, every element is called a divisor, which has the form

$$D = \sum_{p} n_{p} p,$$

where only a finite number of n_p 's are non-zeros. The degree of a divisor is defined as $deg(D) = \sum_p n_p$. Suppose $D_1 = \sum_p n_p p$, $D_2 = \sum_p m_p p$, then $D_1 \pm D_2 = \sum_p (n_p \pm m_p) p$; $D_1 \le D_2$ if and only if for all p, $n_p \le m_p$.

Definition 3.16 (*Meromorphic Function Divisor*). Given a meromorphic function f defined on a Riemann surface S, its divisor is defined as

$$(f) = \sum_{p} \nu_p(f) p.$$

The divisor of a meromorphic differential ω is defined in the similar way.

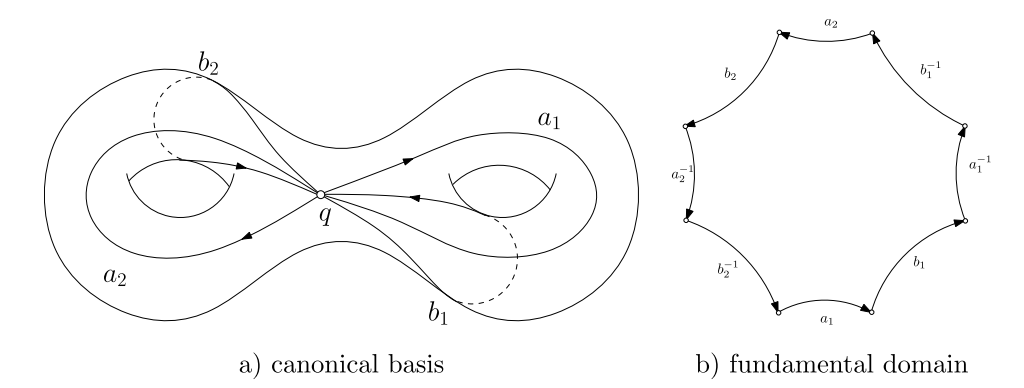


Fig. 4. Canonical fundamental group basis.

Definition 3.17 (*Meromorphic Differential Divisor*). Suppose ω is a meromorphic differential on a Riemann surface S, suppose $p \in S$ is a point on S, we define the order of ω at p as

$$v_p(\omega) = v_p(f_p),$$

where f_p is the local representation of ω in a neighborhood of p, $\omega = f_p(dz_p)^n$.

Definition 3.18 (*Principle Divisor*). The divisors of meromorphic functions are called principle divisors.

All principle divisors are of degree zero. Suppose ω is a meromorphic 1-form, then $deg((\omega)) = 2g - 2$, where g is the genus.

Definition 3.19 (Equivalent Divisors). Two divisors are equivalent, if their difference is a principle divisor.

3.4. Abel-Jacobian theorem

Suppose $\{a_1, b_1, \dots, a_g, b_g\}$ is a set of canonical basis for the homology group $H_1(S, \mathbb{Z})$, each of a_i and b_i represents the curves around the inner and outer circumferences of the *i*th handle. The surface is sliced along the homology group basis to obtain a fundamental domain, as shown in Fig. 4.

Let $\{\omega_1, \omega_2, \dots, \omega_g\}$ be a normalized basis of Ω^1 , the linear space of all holomorphic 1-forms over \mathbb{C} . The choice of basis is dependent on the homology basis chosen above; the normalization signifies that

$$\int_{a_i} \omega_j = \delta_{ij}, \quad i, j = 1, 2, \dots, g.$$

For each curve γ in the homology group, we can associate a vector λ_{γ} in \mathbb{C}^g by integrating each of the g 1-forms over γ ,

$$\lambda_{\gamma} = \left(\int_{\gamma} \omega_1, \int_{\gamma} \omega_2, \dots, \int_{\gamma} \omega_g \right)$$

The *period matrix* of the Riemann surface S is given by:

$$(\lambda_{a_1}, \lambda_{a_2}, \ldots, \lambda_{a_g}; \lambda_{b_1}, \lambda_{b_2}, \ldots, \lambda_{b_g}).$$

We define a 2g-real-dimensional lattice Λ in \mathbb{C}^g ,

$$\Lambda = \left\{ \sum_{i=1}^{g} \alpha_i \ \lambda_{a_i} + \sum_{j=1}^{g} \beta_j \ \lambda_{b_j}, \quad \alpha_i, \beta_j \in \mathbb{Z} \right\}$$

Definition 3.20 (*Jacobian Variety*). The Jacobian Variety of the Riemann surface S, denoted J(S), is the compact quotient \mathbb{C}^g/Λ .

Definition 3.21 (Abel–Jacobi Map). Fix a base point $p_0 \in S$. The Abel–Jacobi map is a map $\mu : S \to J(S)$. For every point $p \in S$, choose a curve γ from p_0 to p inside the fundamental domain; the Abel–Jacobi map μ is defined as follows:

$$\mu(p) = \left(\int_{\gamma} \omega_1, \int_{\gamma} \omega_2, \dots, \int_{\gamma} \omega_g\right) \mod \Lambda,$$

where the integrals are all along γ .

It can be shown $\mu(p)$ is well-defined, that the choice of curve γ does not affect the value of $\mu(p)$. Given a divisor $D = \sum_k n_k p_k$, the Abel–Jacobi map is defined as

$$\mu(D) = \sum_{k} n_k \mu(p_k).$$

Theorem 3.22 (Abel Theorem). Given a compact Riemann surface S of genus g > 0, and a degree zero divisor D, D is a principle divisor if and only if

$$\mu(D) = 0 \quad in \quad J(S). \tag{4}$$

4. Quad-meshes and meromorphic quartic forms

In this section, we show the intrinsic relation between a quad-mesh and a meromorphic quartic differential, this gives the Abel–Jacobi condition for the singularity configuration of any quad-mesh.

4.1. Quadrilateral mesh

Definition 4.1 (Quadrilateral Mesh). Suppose Σ is a topological surface, \mathcal{Q} is a cell partition of Σ , if all cells of \mathcal{Q} are topological quadrilaterals, then we say (Σ, \mathcal{Q}) is a quadrilateral mesh.

On a quad-mesh, the topological valence of a vertex is the number of faces adjacent to the vertex.

Definition 4.2 (Singularity). Suppose (S, Q) is a closed quadrilateral mesh. For each vertex v with topological valence k. If k is 4, then we call v a regular vertex, otherwise a k-singular vertex.

Definition 4.3 (*Quad-mesh Metric*). Suppose (Σ, \mathcal{Q}) is a closed quadrilateral mesh. Each face is treated as a unit planar square, then \mathcal{Q} induces a flat Riemannian metric $\mathbf{g}_{\mathcal{Q}}$ with cone singularities at singularities.

Definition 4.4 (Discrete Curvature). Suppose (Σ, \mathcal{Q}) is a closed quadrilateral mesh. Under the metric $\mathbf{g}_{\mathcal{Q}}$, the discrete curvature at a valence k vertex is

$$\frac{\pi}{2}(4-k)$$
.

Theorem 4.5 (Gauss–Bonnet). Suppose (Σ, \mathcal{Q}) is a closed quadrilateral mesh of genus g. Under the metric $\mathbf{g}_{\mathcal{Q}}$, the total curvature is

$$\sum_{v \in \Omega} \frac{\pi}{2} (4 - k(v)) = 2\pi \chi(\Sigma). \tag{5}$$

4.2. Quad-mesh and meromorphic quartic differential

Theorem 4.6 (Quad-Mesh and Riemann Surface). Suppose (Σ, \mathcal{Q}) is a closed quadrilateral mesh, then the quad-mesh \mathcal{Q} induces a conformal atlas \mathcal{A} , such that (Σ, \mathcal{A}) form a Riemann surface, denoted as $S_{\mathcal{Q}}$.

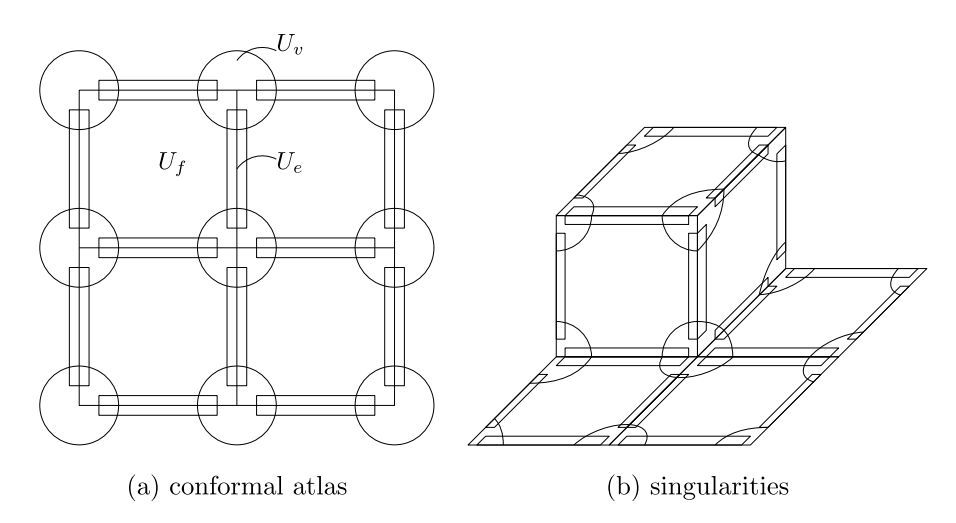


Fig. 5. A quad-mesh induces a conformal atlas, such that the surface becomes a Riemann surface.

Proof. As shown in Fig. 5, we treat each face as the unit Euclidean planar square, this assigns a flat Riemannian metric to the surface, such that the curvature is zero everywhere except at the singularities. At the singularity with valence k, the cone angle is $k\pi/2$.

First, we construct the open covering of the surface. The interior of each face f is one open set U_f ; each edge e is covered by the interior of a rectangle U_e ; each vertex v is covered by a disk, U_v . It is obvious that

$$\Sigma \subset \bigcup_f U_f \bigcup_e U_e \bigcup_v U_v.$$

Second, we establish the local complex parameter of each open set. For each face U_f , we choose the center of the face as the origin, the real and imaginary axises are parallel to the edges of the face, the local parameter is denoted as z_f ; for each edge U_e , we choose the center as the origin, the real axis is parallel to the edge direction, the local parameter is z_e ; for each regular vertex U_v , we choose the center of the disk as the origin, one edge as the real axis, the local parameter is z_v ; for a singular vertex U_v , we first isometrically flatten U_v on the complex plane, to obtain the local parameter w_v , the we use the complex power function to shrink it as

$$w_v^{\frac{4}{k}} \mapsto z_v,$$

where k is valence of the singular vertex.

Now we examine all the coordinate transition maps. We denote a subgroup of the planar rigid motion G generated by

$$z\mapsto e^{i\frac{\pi}{2}}z,\quad z\mapsto z+rac{i}{2},\quad z\mapsto z+rac{i}{2},$$

Then any transition map φ_{fe} between a face and an adjacent edge $z_f \to z_e$ is an element in G, $\varphi_{fe} \in G$; and transition map φ_{ev} between an edge and one of its regular end vertex $z_e \to z_v$ is an element in G, $\varphi_{ev} \in G$.

The transition between a singularly vertex and its neighboring edge or face is more complicated. For example, the transition from a face to its neighboring singular vertex is given by

$$z_{v} = \left(e^{i\frac{n\pi}{2}}z_{f} + \frac{1}{2}(\pm 1 \pm i)\right)^{\frac{2}{k}} \tag{6}$$

where $m, n \in \mathbb{Z}$, k is the valence of v.

Hence all the transition maps are biholomorphic. $\mathcal{A} = \{(U_f, z_f), (U_e, z_e), (U_v, z_v)\}$ form a conformal atlas. (Σ, \mathcal{A}) is a Riemann surface. \square

Theorem 4.7 (Quad-Mesh to Meromorphic Quartic Differential). Suppose (Σ, Q) is a closed quadrilateral mesh, then the quad-mesh Q induces a quartic differential ω_Q on S_Q . The valence-k singular vertices correspond to poles or zeros of order k-4. Furthermore, the trajectories of ω_Q are finite.

Proof. We construct a holomorphic 1-form on each face U_f , dz_f . Because the orientations of all faces are chosen individually, dz_f is not globally defined. Then we define the holomorphic quartic form

$$\omega = (dz_f)^4,$$

then ω is globally defined. Suppose a face f and an edge e are adjacent, then

$$dz_f = e^{i\frac{n\pi}{2}}dz_e, \ n \in \mathbb{Z},$$

then $(dz_f)^4 = (dz_e)^4$. Suppose an edge e has an regular edge vertex v

$$dz_e = e^{i\frac{n\pi}{2}}dz_v, \ n \in \mathbb{Z},$$

therefore $(dz_e)^4 = (dz_v)^4$. Suppose a face f has a regular vertex v, according to Eq. (6), where k = 4,

$$dz_v = e^{i\frac{n\pi}{2}} dz_f,$$

hence $(dz_v)^4 = (dz_f)^4$.

Suppose v is a singular vertex with valence $k \neq 4$, by Eq. (6), we obtain

$$\frac{k}{4}z_v^{\frac{k-4}{4}}dz_v = e^{i\frac{n\pi}{2}}dz_f,$$

therefore

$$\left(\frac{k}{4}\right)^4 z_v^{k-4} (dz_v)^4 = (dz_f)^4 = \omega. \tag{7}$$

Hence, a valence 3 singular vertex corresponds to a simple pole $\frac{c}{z_v}dz_v^4$, a valence 5 singular vertex becomes a simple zero $cz_vdz_v^4$.

Therefore, the meromorphic quartic differential ω is globally defined, the valence-k singular vertices correspond to poles or zeros with order k-4. The finiteness of the trajectories of ω is obvious. \square

Theorem 4.8 (Quartic Differential to Quad-Mesh). Suppose (Σ, A) is a Riemann surface, ω is a meromorphic quartic differential with finite trajectories, then ω induces a quadrilateral mesh \mathcal{Q} , such that the poles or zeros with order k of ω correspond to the singular vertices of \mathcal{Q} with valence k+4.

Proof. The horizontal and vertical trajectories of ω partition the surface into rectangles. Given a pole with local representation

$$\omega = c_1 z^k dz^4,$$

the holomorphic 1-form is given by $\sqrt[4]{\omega}$ with local representation

$$c_2 z^{\frac{k}{4}} dz = \frac{4}{k+4} c_2 d(z^{\frac{k+4}{4}}),$$

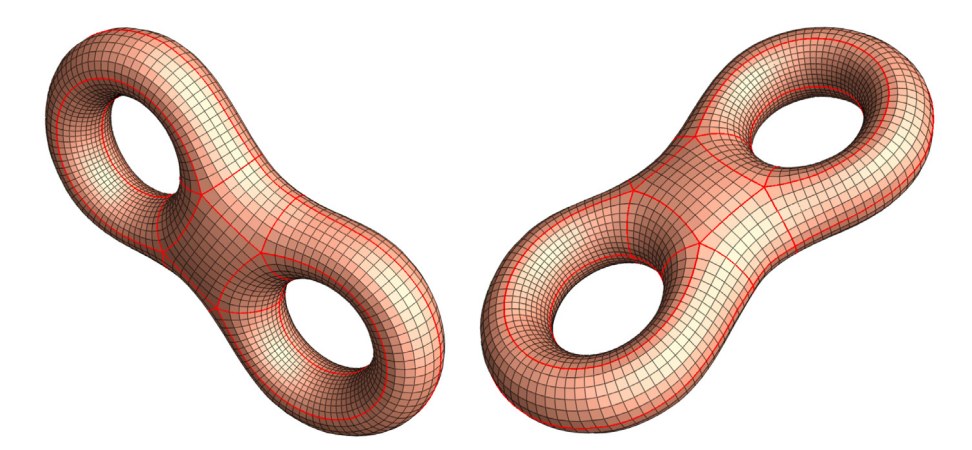
the integration of $\sqrt[4]{\omega}$ maps the 2π angle to $\frac{k+4}{2}\pi$, therefore the valence of the singular vertex equals k+4. \Box Fig. 6 shows the quad-meshes induced by holomorphic differentials.

4.3. Abel-Jacobi condition

Definition 4.9 (Quad-Mesh Divisor). Suppose Q is a closed quadrilateral mesh, ω_Q is the induced meromorphic quartic form. Then the quad-mesh induces a divisor $D_Q = (\omega_Q)$:

$$D_Q = (\omega_Q) = \sum_{v \in Q} (k(v) - 4)v,$$

where k(v) is valence of the vertex v.



quad-mesh induces by a holomorphic quartic differential

Fig. 6. Quadrilateral meshes induced by holomorphic differentials.

Theorem 4.10. Suppose Q is a closed quadrilateral mesh of genus g, the degree of the induced divisor D_Q is $deg(D_Q) = 8g - 8$.

Proof. Directly induced by the Gauss–Bonnet condition of \mathbf{g}_O in Eq. (5). \square

Theorem 4.11 (Quad-mesh Abel–Jacobi condition). Suppose Q is a closed quadrilateral mesh, S_Q is the induced Riemann surface, D_Q is the induced divisor. Assume ω_0 is an arbitrary holomorphic 1-form on S_Q , then

$$\mu(D_O - 4(\omega_0)) = 0 \tag{8}$$

in the Jacobian $J(S_O)$.

Proof. Suppose the meromorphic differential induced by Q is ω_Q . The ratio $f = \omega_Q/\omega_0^4$ is a meromorphic function, therefore according to Abel theorem $\mu((f)) = 0$ in $J(S_Q)$,

$$\mu((f)) = \mu((\omega_Q/\omega_0^4)) = \mu((\omega_Q) - (\omega_0^4)) = \mu(D_Q - 4(\omega_0)) = 0 \quad \mod \Gamma.$$

in $J(S_O)$. \square

Namely, the divisors of all meromorphic differentials are equivalent, and are mapped to the same point in $J(S_Q)$ by the Abel–Jacobi map.

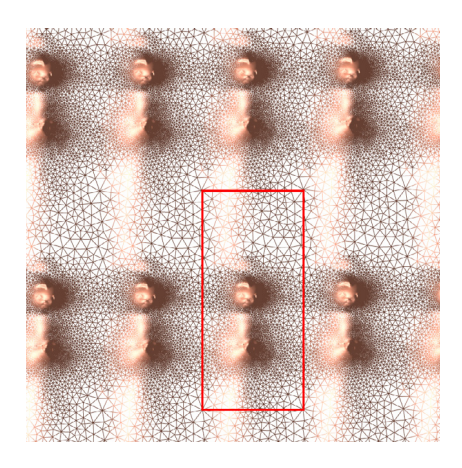
Corollary 4.12. A quadrilateral mesh Q on a genus one surface with only one valence 3 and one valence 5 singularity cannot exist.

Proof. Suppose p is the valence 3 singularity, q is the valence 5 singularity. Then p is the simple pole of ω_Q , q is the simple zero of ω_Q . Suppose ω_0 is the canonical holomorphic 1-form on the Riemann surface S_Q . $\{a,b\}$ is a set of canonical homology group basis, Ω is a fundamental domain (see Fig. 7). Choose a base point $p_0 \in \Omega$ and paths $\gamma_p, \gamma_q \subset \Omega$, connecting the base point to the pole and the zero. According to Abel–Jacobi condition in Eq. (8),

$$\mu(p-q) = \int_{\gamma_p} \omega_0 - \int_{\gamma_q} \omega_0 = 0,$$

therefore the pole p and the zero q coincide, name the valence 3 and valence 5 vertices coincide. Contradiction, hence such kind of Q does not exist. \square





- (a) a holomorphic 1-form ω_0
- (b) a fundamental domain Ω

Fig. 7. The proof of Corollary 4.12 based on Abel–Jacobi condition Theorem 4.11. No genus one closed quad-mesh has only one valence 3 and one valence 5 singular vertices.

According to the Abel-Jacobi theorem, there exists quadrilateral mesh Q on a genus one surface with only one valence 2 and one valence 6 singularity. Suppose S_Q is a torus, with one zero p of order 2 and one pole q of order -2. Suppose the fundamental group generators of the Riemann surface S_Q are a and b, ω is a holomorphic 1-form, such that the integration of ω along a and b are 1 and a respectively. Then according to Abel theorem

$$2[J(p) - J(q)] = 2\left[\int_{\gamma_p} \omega - \int_{\gamma_q} \omega\right] \equiv 0 \mod \{\alpha + \beta z | \alpha, \beta \in \mathbb{Z}\}.$$

 Ω is a fundamental domain and the integration of ω along a and b are 1 and z. It is possible to find two points p, q satisfy

$$\int_{\gamma_n} \omega - \int_{\gamma_n} \omega = \frac{1}{2} + \frac{z}{2}.$$

The key difference with Corollary 4.12 is the orders of the pole and zero. Suppose S is a torus, the fundamental group generators of the Riemann surface S are a and b, ω is a holomorphic 1-form, such that the integration of ω along a and b are 1 and z respectively. Ω is the fundamental domain. We can easily find two points \tilde{p} , $\tilde{q} \in \Omega$ satisfying $\tilde{p} - \tilde{q} = \frac{1}{2} + \frac{z}{2}$, and there is no such points satisfying $\tilde{p} - \tilde{q} = 1 + z$. Fig. 8 shows an Annulus whose double cover is a torus with quad mesh of singularities of degree 2 and 6 only.

Theorem 4.13 (Inverse Theorem of Abel–Jacobi Condition). Suppose S is a compact Riemann surface of genus g, ω_0 is a holomorphic one-form, D is a divisor, satisfying

$$\mu(D - 4(\omega_0)) = 0 \tag{9}$$

in J(S), then there exists a meromorphic quartic differential ω , such that $(\omega) = D$.

Proof. According to Abel theorem, $\mu(D-4(\omega_0))=0$ in J(S) implies there exists a meromorphic function f, such that $(f)=D-4(\omega_0)$, then let

$$\omega = f \cdot \omega_0^4$$

then $(\omega) = (f) + (\omega_0^4) = D$ is the desired meromorphic quartic differential. \square

¹ This example is provided by Kendrick Shepherd and we check its Abel-Jacobi condition in the next section.

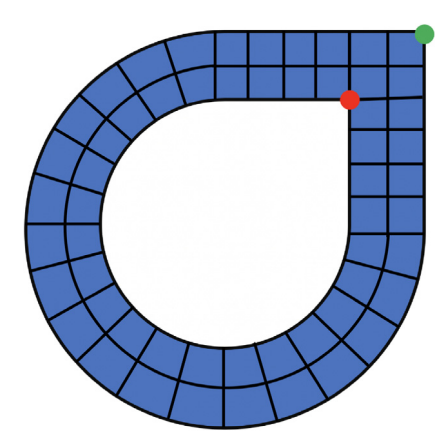


Fig. 8. An Annulus whose double cover is a torus with order 2 zero and order -2 pole only.

Corollary 4.14. Suppose S is a compact Riemann surface of genus g, ω_0 is a holomorphic one-form, D is a divisor, satisfying condition in Eq. (9) in J(S), then there exists a meromorphic quartic differential ω , such that $(\omega) = D$. Furthermore, if the trajectories of ω are finite, then ω induces a quadrilateral mesh Q.

Proof. The surface can be sliced along the trajectories of ω , especially those through the zeros and poles. This produces a quadrilateral mesh. \square

5. Computational algorithms

This section explains the computational algorithms to verify Abel–Jacobi condition and construct meromorphic quartic differentials in detail.

5.1. Abel-Jacobi condition verification

Given a closed triangle mesh, and a divisor, we would like to verify if the divisor satisfies the Abel–Jacobi condition. This involves the computation of the canonical basis for the homology group and holomorphic differential group. The canonical homology group basis is carried out using the geometry-aware handle loop and tunnel loop algorithm in [30]. the holomorphic differential basis is computed using the algorithm described in [31]. The computation of the period matrix and Abel–Jacobi map is straight forward. The details of the algorithm are described in Alg. 1.

Genus one cases. This elk model in Fig. 9 is a genus one surface. The left frame shows the quad-mesh Q, the right frame shows the holomorphic 1-form ω_0 . The induced meromorphic quartic differential ω_Q has 26 poles and 26 zeros,

$$D_Q = (\omega_Q) = \sum_{i=1}^{26} (p_i - q_i).$$

The results of the Abel-Jacobi map are as follows:

$$\mu\left(\sum_{i=1}^{26} p_i\right) = 5.8952427 + i2.7571920, \quad \mu\left(\sum_{j=1}^{26} q_j\right) = 5.8954460 + i2.7571919.$$

Therefore, $\mu(D_Q)$ is the difference between them, which is -2.03332e - 04 + i1.044e - 07, very close to the theoretic prediction (0, 0).

Fig. 10 shows another genus one model, the rocker-arm. The left frame shows the quad-mesh Q, the right frame shows the holomorphic 1-form ω_0 . The induced meromorphic quartic differential has 18 poles and 18 zeros.

$$D_Q = \sum_{i=1}^{18} (p_i - q_i),$$

Algorithm 1: Abel Condition Verification

Input: Closed Surface S of genus g > 0; Divisor D

Output: Whether D satisfies Abel Condition

- 1 if $deg(D) \neq 8g 8$ then return false;
- 2 Compute the canonical homology group generators $\{a_1, \ldots, a_g; b_1, \ldots, b_g\}$;
- 3 Compute the dual holomorphic 1-form basis $\{\omega_1, \dots, \omega_g\}$;
- 4 Compute the period matrix of S and obtain its submatrices A, B;
- 5 Compute the Abel-Jacobi map $\mu(D)$;
- 6 Solve equation group

$$(\operatorname{Img} B)\beta = \operatorname{Img}\mu(D),$$

to obtain
$$\beta = (\beta_1, \beta_2, \dots, \beta_g)^T$$
.

7 Solve equation group

$$A\alpha = \mu(D) - B\beta$$

to obtain $\alpha = (\alpha_1, \alpha_2, \dots, \alpha_g)^T$.

8 if all α_i 's and β_j 's are integer then return true; otherwise return false.

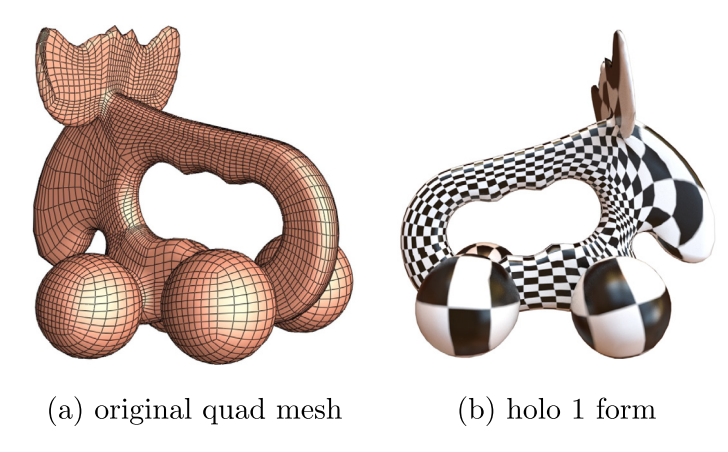


Fig. 9. The genus 1 elk model.

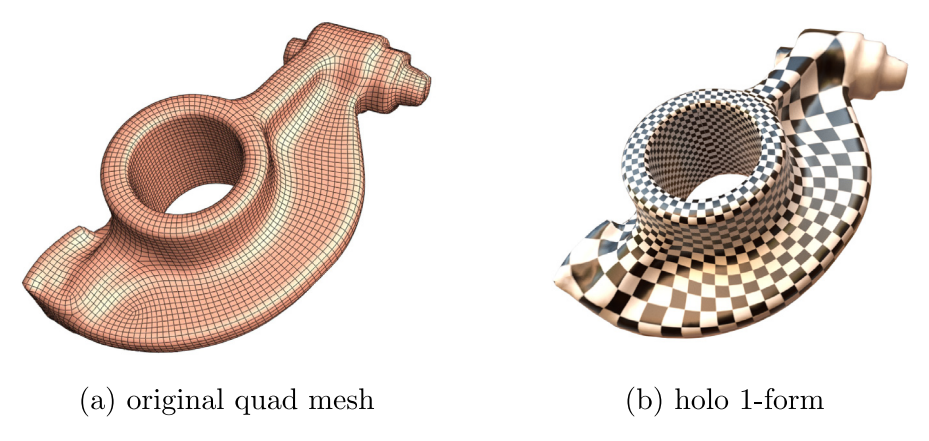
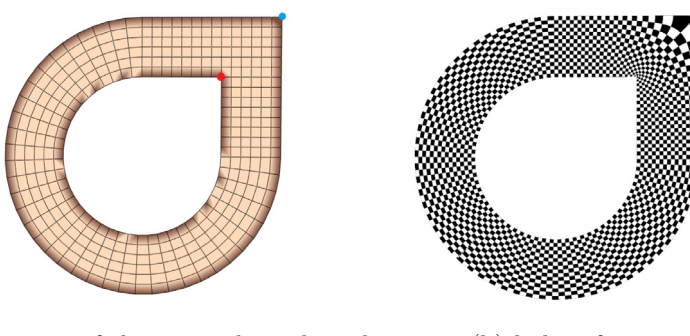


Fig. 10. The genus 1 rockerarm model.



(a) front view of the original quad mesh

(b) holo 1-form

Fig. 11. The genus 1 model which has a quad mesh with degree 2 and 6 singularities only.

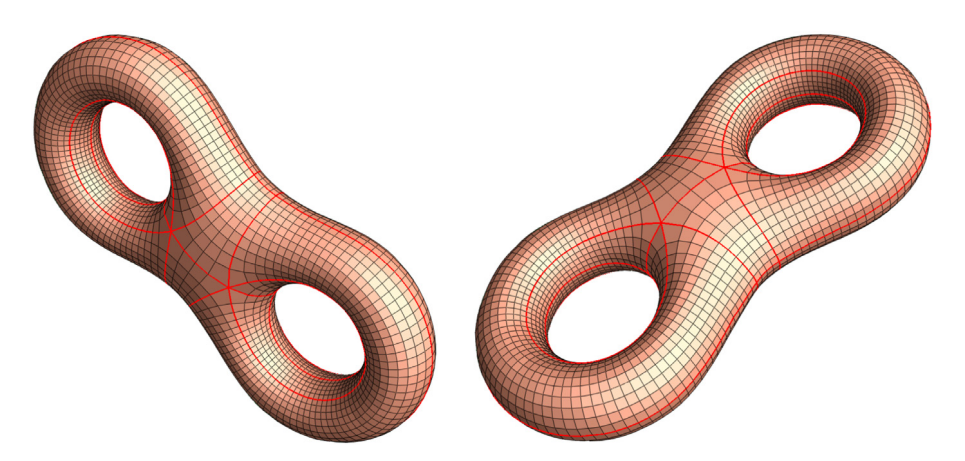


Fig. 12. The input genus two quad-mesh.

The results of the Abel-Jacobi map are as follows:

$$\mu\left(\sum_{j=1}^{18} p_j\right) = 2.61069 + i0.588368, \quad \mu\left(\sum_{i=1}^{18} q_i\right) = 2.61062 + i0.588699.$$

Hence, $\mu(D_Q)$ is the difference between them, which equals 6.967e - 05 - i3.3064e - 4, very close to the origin in $J(S_Q)$.

Fig. 11 shows genus one model with two singularities of degree 2 and 6 only. The left frame shows the quad-mesh Q, the right frame shows the holomorphic 1-form ω_0 . The induced meromorphic quartic differential has 1 pole q_0 of order -2 and 1 zero p_0 with order 2.

$$D_O = 2 \cdot p_0 - 2 \cdot q_0,$$

Suppose the fundamental group generators of the Riemann surface S_Q are a and b, we can compute the integration of ω_0 along a and b are 1 and i4.75524 respectively. Hence The results of the Abel–Jacobi map are as follows:

$$\mu(D_Q) = \mu(2 \cdot p_0 - 2 \cdot q_0)$$

$$= 2 \cdot (0.5 + i9.3678e - 15) - 2 \cdot (0 + i0)$$

$$= 1 + i1.87356e - 14$$

$$\equiv 0 + i3.94e - 15 \mod 1 + i4.75524$$

which is vary close to the origin in $J(S_Q)$.

Genus two case. Fig. 12 shows a genus two quad-mesh Q, which has four order two zeros. Fig. 13 shows the homology group basis of the mesh, the tunnel loops a_0 , a_1 and the handle loops b_0 , b_1 . Fig. 14 shows holomorphic



(a) tunnel loops (b) handle loops

Fig. 13. The homology group basis.

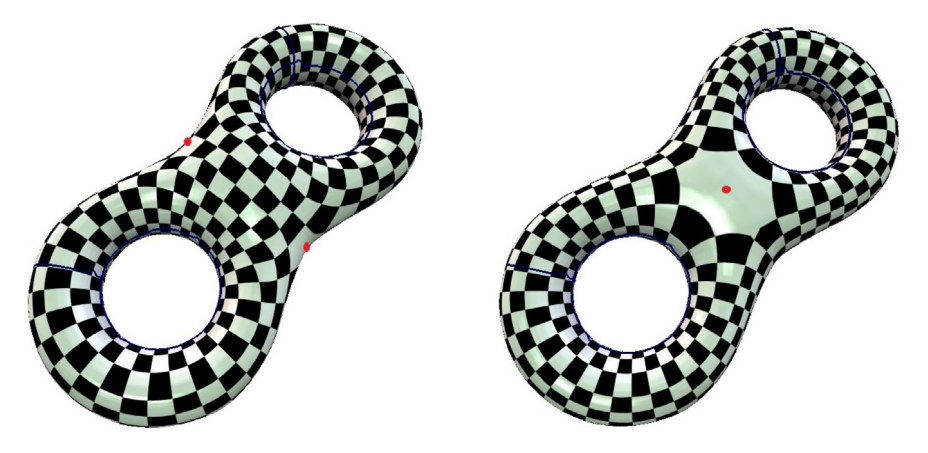


Fig. 14. The holomorphic differential basis.

differential basis φ_0 and φ_1 computed under the quad-mesh metric \mathbf{g}_Q . We set φ_0 as ω_0 and verify the Abel–Jacobi condition by computing the Abel–Jacobi map $\mu(D_Q - 4(\omega_0))$. The period matrix A of the Riemann surface S_Q is

$$\begin{pmatrix} 0.99999999 - i1.4209e - 09 & 0.99999989 - i6.01812e - 08 \\ 1 + i1.24783e - 08 & 1.9999998 - i9.03562e - 08 \end{pmatrix}$$

The period matrix B is

$$\begin{pmatrix} 3.18e - 08 + i0.38191542 & 4.7433845e - 20 + i0.3861979 \\ 1.04e - 08 + i0.35091173 & 1.1519648e - 19 + i0.80339934 \end{pmatrix}$$

Matrix BA^T is symmetric, with imaginary part positive defined and the basis satisfying the Riemann Bilinear Relation:

$$BA^{T} = \begin{pmatrix} 5.5584516e - 08 + i0.76811328 & 6.1929719e - 08 + i1.1543112 \\ 5.9248147e - 08 + 1.154311 & 7.861333e - 08 + i1.9577103 \end{pmatrix}$$

$$AB^{T} - BA^{T} = \begin{pmatrix} 0 & -2.6815727e - 09 - i1.843294e - 07 \\ 2.6815727e - 09 + i1.843294e - 07 & 0 \end{pmatrix}$$

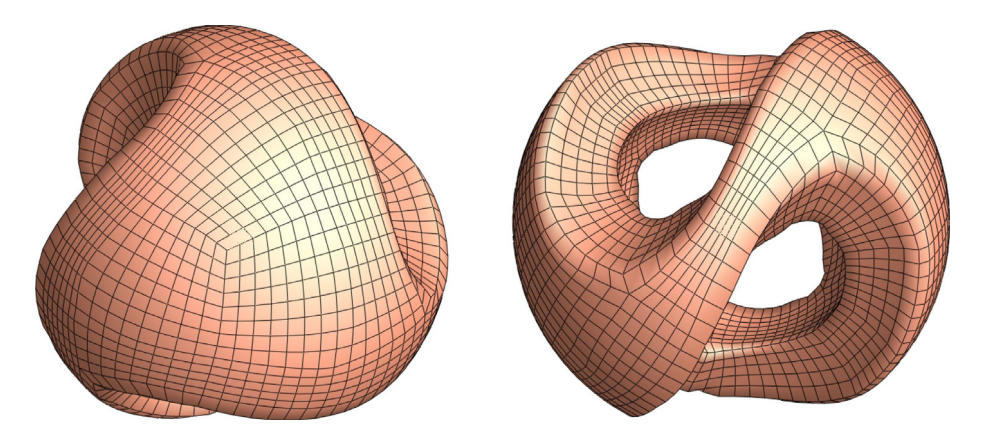


Fig. 15. A genus 2 quad-mesh of a sculpture model.

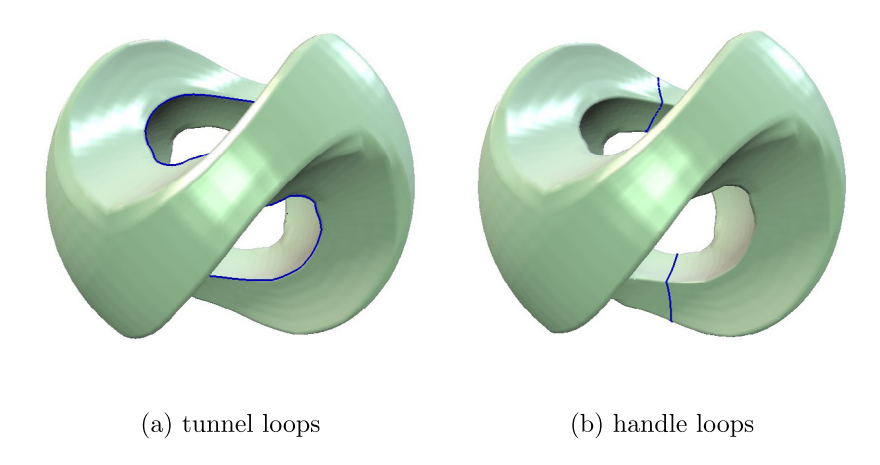


Fig. 16. Tunnel and handle loops of the sculpture model.

The Abel-Jacobi image of the divisor,

$$\mu(D_Q-4(\omega_0)) = \binom{1e-06}{2e-07-i1.6e-06},$$

which is very close to 0. This shows the Abel-Jacobi condition holds for the quad-mesh in Fig. 12.

Fig. 15 shows another genus two quad-mesh of a sculpture model which has 12 valence-5 vertices and 4 valence 3 vertices. Fig. 16 shows the tunnel and handle loops of the sculpture model. Fig. 17 shows the basis of the holomorphic differentials φ_0 and φ_1 .

We set φ_0 as ω_0 and verify the Abel–Jacobi condition by computing the Abel–Jacobi map $\mu(D_Q-4(\omega_0))$. The period matrix A of the Riemann surface S_Q is

$$\begin{pmatrix} 0.99999997 & -i2.8e - 09 & -0.24999994 + i2.745e - 08 \\ 0.99999999 + i1.13e - 08 & 0.50000015 + i4.1e - 08 \end{pmatrix}.$$

The period matrix B is

$$\begin{pmatrix} -4.8789098e - 19 + i0.50669566 & 7.4538899e - 19 + i0.15720634 \\ -7.5894152e - 19 + i0.73261918 & 4.8789098e - 19 + i0.589281 \end{pmatrix}.$$

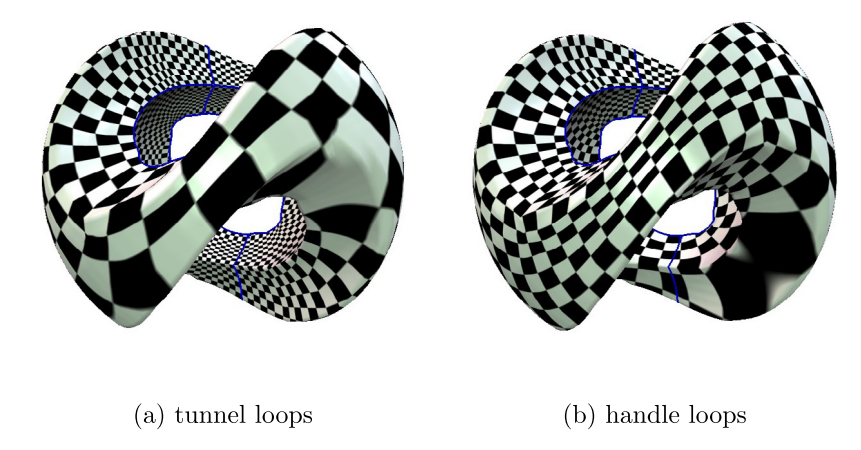


Fig. 17. Holomorphic 1-form basis of the sculpture model.

Matrix BA^T is symmetric, with imaginary part positive defined and the basis satisfying the Riemann Bilinear Relation:

$$BA^{T} = \begin{pmatrix} -2.8965662e - 09 + i0.46739407 & -1.2171121e - 08 + i0.58529885 \\ -1.412443e - 08 + i0.58529895 & -3.2439118e - 08 + i1.0272598 \end{pmatrix}$$

$$AB^{T} - BA^{T} = \begin{pmatrix} 0 & -1.9533089e - 09 + i9.7987673e - 08 \\ 1.9533089e - 09 - i9.7987673e - 08 \end{pmatrix}$$

The Abel-Jacobi map image of the divisor is

$$\mu(D_{\mathcal{Q}}-4(\omega_0)) = \begin{pmatrix} -1.568599999979e - 05 + i3.69999999994e - 06 \\ 4.2889999998e - 05 - i4.400000000182e - 07 \end{pmatrix},$$

which is very close the 0.

5.2. Meromorphic quartic differential construction

In practice, a surface Σ embedded in \mathbb{R}^3 is given, the induced Euclidean metric is \mathbf{g} . Our purpose is to construct a quadrilateral mesh \mathcal{Q} on (Σ, \mathbf{g}) . It is highly desirable that the metric induced by \mathcal{Q} , $\mathbf{g}_{\mathcal{Q}}$, is conformal equivalent to the original metric \mathbf{g} . From above discussion, we see the equivalence between a quad-mesh \mathcal{Q} and the meromorphic quartic differential $\omega_{\mathcal{Q}}$ on the Riemann surface $S_{\mathcal{Q}}$. Therefore $\omega_{\mathcal{Q}}$ is also a meromorphic differential on (Σ, \mathbf{g}) .

Suppose (Σ, \mathbf{g}) is a genus zero closed surface, then it is conformal equivalent to the unit sphere \mathbb{S}^2 , namely $\mathbb{C} \cup \{\infty\}$. The unit sphere \mathbb{S}^2 has two charts z and w, z covers \mathbb{C} , w covers $\mathbb{C} \cup \{\infty\} \setminus \{0\}$, the transition map is w = 1/z. We define the simplest meromorphic differential

$$\omega_0 = dz = -\frac{1}{w^2} dw.$$

Given a quad-mesh $\mathcal Q$ on $\mathcal \Sigma$, then $f=\omega_{\mathcal Q}/w_0^4$ is a meromorphic function. On the sphere, any meromorphic function is a rational function, the general global representation of $\omega_{\mathcal Q}$ on $\mathbb C$ is given by:

$$\omega_Q = \frac{(z - p_1)(z - p_2) \cdots (z - p_{n-8})}{(z - q_1)(z - q_2) \cdots (z - q_n)} dz^4, \tag{10}$$

where $\{p_1, p_2, \ldots, p_{n-8}\}$ are the simple zeros, $\{q_1, q_2, \ldots, q_n\}$ are the simple poles of ω_Q . The ∞ point is the zero of order 8. Each simple zero corresponds to a valence 5 vertex, each simple pole corresponds to a valence 3 vertex. The zeros (poles) can be merged into high order ones, thus Eq. (10) becomes

$$\omega_{Q} = \frac{\prod_{i=1}^{k} (z - p_{i})^{n_{i}}}{\prod_{i=1}^{l} (z - q_{i})^{m_{i}}} dz^{4}, \tag{11}$$

where $\sum_{j=1}^{l} m_j - \sum_{i=1}^{k} = 8$, m_i 's and n_j 's are positive integers.

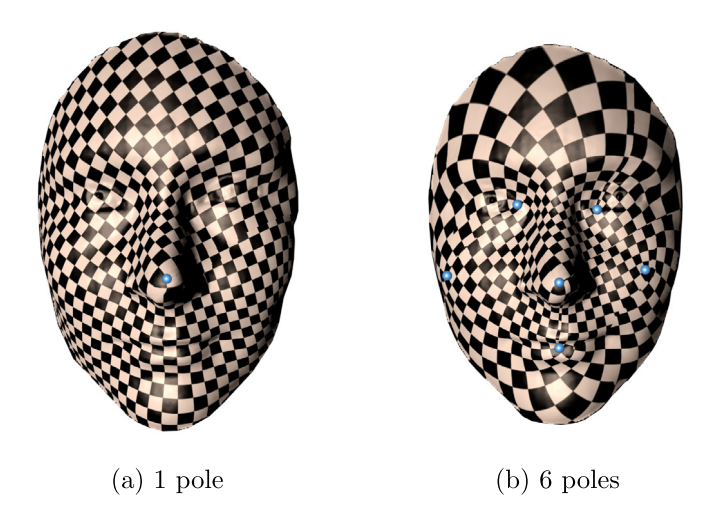


Fig. 18. The visualization of meromorphic quartic differential on a face model.

Table 1 Poles in the meromorphic differential Eq. (12).

$z_1 = 0.451559 + 0.21962i$	$z_2 = 0.45696 + 0.617636i$	$z_3 = 0.706853 + 0.52086i$
$z_4 = 0.533522 + 0.407822i$	$z_5 = 0.250598 + 0.471244i$	$z_6 = 0.747474 + 0.28336i$

Eqs. (10) and (11) give all possible meromorphic quartic differentials on the sphere, some of them have infinite trajectories. The ones with finite trajectories correspond to ω_Q for some quad-mesh Q.

Fig. 18 left frame shows two different meromorphic quartic differentials constructed in this way. In the left frame, we compute a Riemann mapping to conformally map the facial surface S onto the planar unit disk using the method in [2], then pick a pole $z_1 = 0.706853 + 0.52086i$. The meromorphic quartic differential is given by

$$\omega = \frac{1}{z - z_1} (dz)^4.$$

The we find a path γ from z_1 to the boundary, slice the surface along γ to get a simply connected domain \bar{S} . In this domain, we choose one branch of $\sqrt[4]{\omega}$. By integrating $\sqrt[4]{\omega}$ on \bar{S} , we map \bar{S} onto the complex plane. Then we use checkerboard texture mapping to visualize the trajectories of ω .

Fig. 18 right frame demonstrates a meromorphic quartic differential with 6 poles,

$$\omega = \frac{1}{\prod_{i=1}^{6} (z - z_i)} (dz)^4 \tag{12}$$

where the poles are given in Table 1.

We compute a cut graph γ connecting all the singularities and the boundary using the algorithm in [32], then slice the surface along γ to get a simply connected domain \bar{S} . By integrating a branch of $\sqrt[4]{\omega}$, we map \bar{S} onto the complex plane. Any branch can be used as long as it is continuous on \bar{S} and one branch is enough because we adopt complex integration.

Fig. 19 shows a meromorphic quartic differential with 4 poles and 2 zeros,

$$\omega = \frac{(z - p_1)(z - p_2)}{\prod_{i=1}^{6} (z - q_i)} (dz)^4,$$
(13)

where the poles and zeros are given in Table 2.

Fig. 20 demonstrates a meromorphic quartic differential on the Max Planck head model. First, we conformally map the model onto the unit sphere using the algorithm in [33], then the sphere is mapped onto the complex

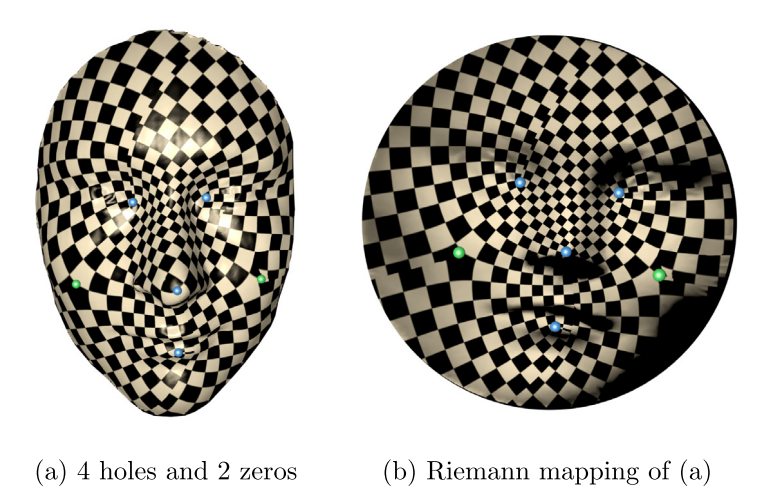


Fig. 19. The visualization of meromorphic quartic differential on a face model.

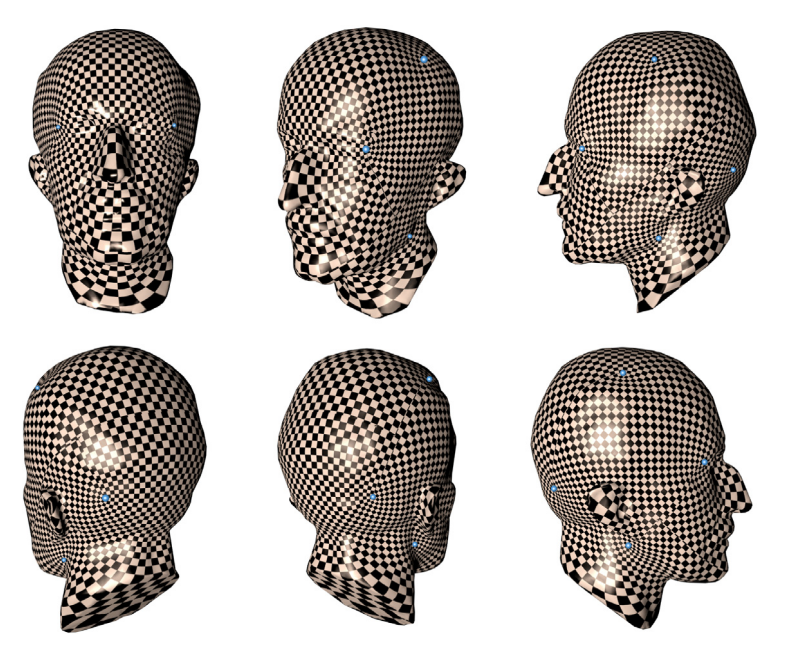


Fig. 20. A meromorphic quartic differential on the Max-Planck sculpture model with 8 poles.

The zeros and poles in the meromorphic differential in Eq. (13).

$p_1 = 0.250598 + 0.471244i$	$p_2 = 0.747474 + 0.28336i$	$q_1 = 0.451559 + 0.21962i$		
$q_2 = 0.45696 + 0.617636i$	$q_3 = 0.706853 + 0.52086i$	$q_4 = 0.533522 + 0.407822i$		

plane using the stereo-graphic projection. On the complex plane, we construct a meromorphic quartic differential as (see Fig. 21)

$$\omega = \frac{1}{\prod_{i=1}^{8} (z - q_i)} (dz)^4, \tag{14}$$

where the poles are given in Table 3.

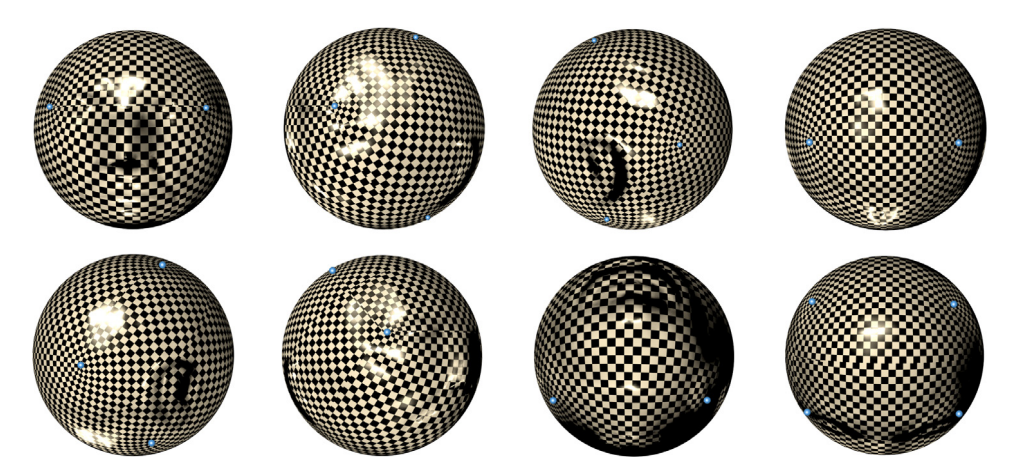


Fig. 21. The meromorphic quartic differential the conformal spherical image of the Max-Planck sculpture model with 8 poles.

Table 3The poles of the meromorphic differential on Max Planck head model in Eq. (14).

$q_1 = 1.32607 + 1.3106i$	$q_2 = -1.27859 + 1.27903i$	$q_3 = 1.30017 - 1.25335i$
$q_4 = -1.29695 - 1.28728i$	$q_5 = 0.471821 - 0.46131i$	$q_6 = -0.443743 - 0.468551i$
$q_7 = 0.452511 + 0.463833i$	$q_8 = -0.450766 + 0.468879i$	

Table 4The zeros and poles of the meromorphic differential on the Max Planck head model in Eq. (15).

$p_1 = 0.898261 + 3.24367i$	$p_2 = -0.00810208 - 0.25253i$	$q_1 = 0.00289177 + 0.255035i$
$q_2 = 1.03926 - 3.32305i$	$q_3 = 1.5921 + 0.915034i$	$q_4 = -1.61079 + 0.858346i$
$q_5 = 1.61098 - 0.845895i$	$q_6 = -1.63865 - 0.894138i$	$q_7 = 0.559829 + 0.296053i$
$q_8 = -0.564592 + 0.307631i$	$q_9 = 0.555884 - 0.307683i$	$p_{10} = -0.550573 - 0.311611i$

Similarly, a cut graph γ connecting all singularities is computed, the surface is sliced along the cut graph to get a simply connected domain. We integrate $\sqrt[4]{\omega}$ on the domain, to flatten the surface to the complex plane. By checkerboard texture mapping, the trajectories of ω can be visualized.

The second meromorphic quartic differential is shown in Fig. 22, which has the form on the complex plane (see Fig. 23)

$$\omega = \frac{\prod_{i=1}^{2} (z - p_i)}{\prod_{i=1}^{8} (z - q_i)} (dz)^4,$$
(15)

where the zeros and the poles are given in Table 4.

6. Conclusion

This work proves the equivalence between quadrilateral meshes and meromorphic quartic differentials on Riemann surfaces with finite trajectories (Theorems 4.7 and 4.8); Second, this work gives Abel–Jacobi condition for the configurations of singularities of quad-meshes (Theorem 4.11), the condition can be easily verified algorithmically; Third, the meromorphic quartic differentials can be constructed on surfaces using their global algebraic representation, this leads to a novel direction for quad-mesh generation based on meromorphic differentials. Our experimental results demonstrate that the method is theoretically rigorous, practically simple and efficient. This opens a new direction for quad-mesh generation based on Riemann surface theory.

In future, we will explore the methods to guarantee the finiteness of all the trajectories of meromorphic differentials, the algorithm for divisor optimization to satisfy the Abel–Jacobi condition and generalize the Abel–Jacobi condition to hexahedral meshes.

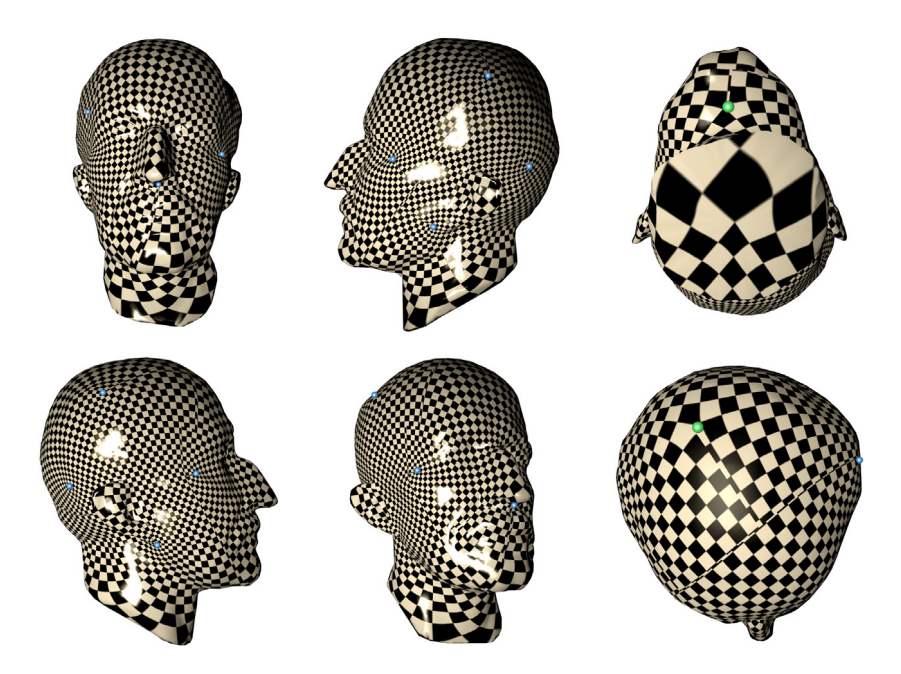


Fig. 22. A meromorphic quartic differential on the Max-Planck sculpture model with 10 poles (blue) and 2 zeros (green). (For interpretation of the references to color in this figure legend, the reader is referred to the web version of this article.)

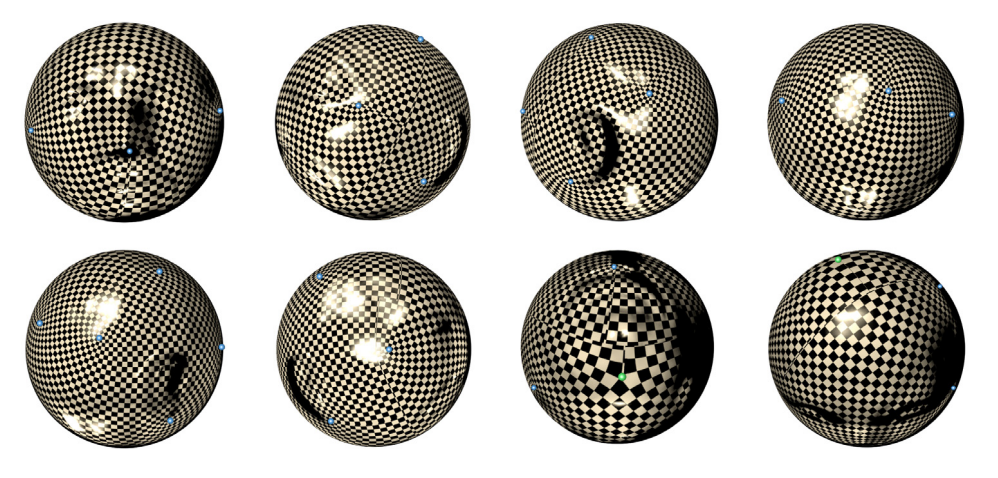


Fig. 23. The meromorphic quartic differential the conformal spherical image of the Max-Planck sculpture model with 10 poles and 2 zeros.

Declaration of competing interest

The authors declare that they have no known competing financial interests or personal relationships that could have appeared to influence the work reported in this paper.

Acknowledgments

This work is partially supported by National Natural Science Foundation of China (Grant No. 61720106005, No. 61772105, No. 61907005, No. 61936002), the National Science Foundation of the United States (Grant No. CMMI-1762287, DMS-1737812).

References

- [1] Wei Chen, Xiaopeng Zheng, Jingyao Ke, Na Lei, Zhongxuan Luo, Xianfeng Gu, Quadrilateral mesh generation I: Metric based method, Comput. Methods Appl. Mech. Eng. 356 (2019) 652–668.
- [2] Xianfeng David Gu, Feng Luo, Jian Sun, Tianqi Wu, A discrete uniformization theorem for polyhedral surfaces, J. Differential Geom. (JDG) 109 (2) (2018) 223–256.
- [3] Ashis Myles, Nico Pietroni, Denis Zorin, Robust field-aligned global parametrization, ACM Trans. Graph. 33 (4) (2014) 135:1–135:14.
- [4] David Bommes, Bruno Lévy, Nico Pietroni, Enrico Puppo, Claudio Silva, Marco Tarini, Denis Zorin, Quad-mesh generation and processing: A survey, Comput. Graph. Forum 32 (6) (2013) 51–76.
- [5] Topraj Gurung, Daniel Laney, Peter Lindstrom, Jarek Rossignac, Squad: Compact representation for triangle meshes, Comput. Graph. Forum 30 (2) (2011) 355–364.
- [6] J.F. Remacle, J. Lambrechts, B. Seny, E. Marchandise, A. Johnen, C. Geuzainet, Blossom-quad: A non-uniform quadrilateral mesh generator using a minimum-cost perfect-matching algorithm, Internat. J. Numer. Methods Engrg. 89 (9) (2012) 1102–1119.
- [7] Tarini Marco, Pietroni Nico, Cignoni Paolo, Panozzo Daniele, Puppo Enrico, Practical quad mesh simplification, Comput. Graph. Forum 29 (2) (2010) 407–418.
- [8] Luiz Velho, Denis Zorin, 4-8 Subdivision, Elsevier Science Publishers B.V., 2001.
- [9] Ioana Boier-Martin, Holly Rushmeier, Jingyi Jin, Parameterization of triangle meshes over quadrilateral domains, in: Acm International Conference Proceeding Series, 2004, pp. 193–203.
- [10] Nathan A. Carr, Jared Hoberock, Keenan Crane, John C. Hart, Rectangular multi-chart geometry images, in: Eurographics Symposium on Geometry Processing, 2006, pp. 181–190.
- [11] Jiazhil Xia, Ismael Garcia, Ying He, Shi Qing Xin, Gustavo Patow, Editable polycube map for gpu-based subdivision surfaces, in: Symposium on Interactive 3D Graphics and Games, 2011, pp. 151–158.
- [12] Hongyu Wang, Miao Jin, Ying He, Xianfeng Gu, Hong Qin, User-controllable polycube map for manifold spline construction, in: ACM Symposium on Solid and Physical Modeling, Stony Brook, New York, Usa, June, 2008, pp. 397–404.
- [13] Juncong Lin, Xiaogang Jin, Zhengwen Fan, Charlie C.L. Wang, Automatic polycube-maps, in: International Conference on Advances in Geometric Modeling and Processing, 2008, pp. 3–16.
- [14] Ying He, Hongyu Wang, Chi Wing Fu, Hong Qin, A divide-and-conquer approach for automatic polycube map construction, Comput. Graph. 33 (3) (2009) 369–380.
- [15] Shen Dong, Peer Timo Bremer, Michael Garland, Valerio Pascucci, John C. Hart, Spectral surface quadrangulation, in: ACM SIGGRAPH, 2006, pp. 1057–1066.
- [16] Jin Huang, Muyang Zhang, Jin Ma, Xinguo Liu, Leif Kobbelt, Hujun Bao, Spectral quadrangulation with orientation and alignment control, ACM Trans. Graph. 27 (5) (2008) 1–9.
- [17] Y. Tong, P. Alliez, D. Cohen-Steiner, M. Desbrun, Designing quadrangulations with discrete harmonic forms, in: Eurographics Symposium on Geometry Processing, Cagliari, Sardinia, Italy, June, 2006, pp. 201–210.
- [18] Pierre Alliez, Bruno Lévy, Alla Sheffer, Nicolas Ray, Ray periodic global parameterization, ACM Trans. Graph. 25 (4) (2006) 1460–1485.
- [19] Feli Kälberer, Matthias Nieser, Konrad Polthier, Quadcover surface parameterization using branched coverings, Comput. Graph. Forum 26 (3) (2010) 375–384.
- [20] Bruno Lévy, Yang Liu, Lp centroidal voronoi tessellation and its applications, ACM Trans. Graph. 29 (4) (2010) 1-11.
- [21] Jonathan Palacios, Eugene Zhang, Rotational symmetry field design on surfaces, ACM Trans. Graph. 26 (3) (2007) 55.
- [22] Wan-Chiu Li, Bruno Vallet, Nicolas Ray, Bruno Lévy, Representing higher-order singularities in vector fields on piecewise linear surfaces, IEEE Trans. Vis. Comput. Graphics 12 (5) (2006) 1315–1322.
- [23] Nicolas Kowalski, Franck Ledoux, Pascal Frey, A pde based approach to multidomain partitioning and quadrilateral meshing, in: International Meshing Roundtable, 2013.
- [24] T. Jiang, X. Fang, J. Huang, H. Bao, Y. Tong, M. Desbrun, Frame field generation through metric customization, ACM Trans. Graph. 34 (4) (2015) 1–11.
- [25] Nicolas Ray, Dmitry Sokolov, Robust polylines tracing for n-symmetry direction field on triangulated surfaces, ACM Trans. Graph. (2014).
- [26] Ryan Viertel, Braxton Osting, An approach to quad meshing based on harmonic cross-valued maps and the ginzburg-landau theory, 2017.
- [27] Na Lei, Xiaopeng Zheng, Jian Jiang, Yu Yao Lin, David Xianfeng Gu, Quadrilateral and hexahedral mesh generation based on surface foliation theory, Comput. Methods Appl. Mech. Eng. 316 (2017) 758–781.
- [28] Na Lei, Xiaopeng Zheng, Hang Si, Zhongxuan Luo, Xianfeng Gu, Generalized regular quadrilateral mesh generation based on surface foliation, Procedia Eng. 203 (2017) 336–348.
- [29] Lars V. Ahlfors, Leo Sario, Riemann surfaces, Math. Gaz. 47 (359) (1963).
- [30] Tamal K. Dey, Kuiyu Li, Jian Sun, David Cohen-Steiner, Computing geometry-aware handle and tunnel loops in 3d models, ACM Trans. Graph. 27 (3) (2008) 45:1–45:9.
- [31] Xianfeng Gu, Shing-Tung Yau, Global conformal surface parameterization, in: Proceedings of the 2003 Eurographics/ACM SIGGRAPH Symposium on Geometry Processing, Eurographics Association, 2003, pp. 127–137.
- [32] Xiaokang Yu, Na Lei, Yalin Wang, Xianfeng Gu, Intrinsic 3D dynamic surface tracking based on dynamic ricci flow and teichmüller map, in: 2017 IEEE International Conference on Computer Vision (ICCV), 2017.
- [33] Xianfeng Gu, Yalin Wang, Tony F. Chan, Paul M. Thompson, Shing-Tung Yau, Genus zero surface conformal mapping and its application to brain surface mapping, IEEE Trans. Med. Imaging 23 (8) (2004) 949–958.